Hindawi Publishing Corporation
Mathematical Problems in Engineering
Volume 2015, Article ID 391569, 10 pages
http://dx.doi.org/10.1155/2015/391569

Research Article

Evaluation of Seismic Fragility of Weir Structures in South Korea

Bu Seog Ju[1] and WooYoung Jung[2]

[1]*Institute for Disaster Prevention, Gangneung-Wonju National University, Gangneung 210-702, Republic of Korea*
[2]*Department of Civil Engineering, Gangneung-Wonju National University, Gangneung 210-702, Republic of Korea*

Correspondence should be addressed to WooYoung Jung; woojung@gwnu.ac.kr

Received 3 September 2014; Accepted 2 February 2015

Academic Editor: Valder Steffen Jr.

In order to reduce earthquake damage of multifunctional weir systems similar to a dam structure, this study focused on probabilistic seismic risk assessment of the weir structure using the fragility methodology based on Monte Carlo simulation (MCS), with emphasis on the uncertainties of the seismic ground motions in terms of near field induced pulse-like motions and far field faults. The 2D simple linear elastic plain strain finite element (FE) model including soil structure foundations using tie connection method in ABAQUS was developed to incorporate the uncertainty. In addition, five different limit states as safety criteria were defined for the seismic vulnerability of the weir system. As a consequence, the results obtained from multiple linear time history analyses revealed that the weir structure was more vulnerable to the tensile stress of the mass concrete in both near and far field ground motions specified earthquake hazard levels. In addition, the system subjected to near field motions was primarily more fragile than that under far field ground motions. On the other hand, the probability of failure due to the tensile stress at weir sill and stilling basin showed the similar trend in the overall peak ground acceleration levels.

1. Introduction

Recently 16 multifunctional weir structures were constructed on four major rivers in Korea. Weir structures designed to change river flow characteristics have similar functions like dams such as electric power generation, flooding control, and water supply. While there are many advantages associated with weir structures, they also have weaknesses; few weaknesses were reported in the case of weir structures built in the rivers. In another word, the weir structure is one of the infrastructures that have coexisting pros and cons. The general examples of drawbacks include increase of the oxygen content, accumulating garbage and other debris, and fauna changes in the water (http://en.wikipedia.org/wiki/Weir). Furthermore, the weir structures can be exposed to multiple hazards such as earthquakes and flooding caused by serious problems such as flooding due to structural failure, discontinuity between soil foundation and the weir, and strong impulse water wave due to ground motions.

According to Chanson [1], over the past decades, several failures in 20 hydraulic structures (dams and weirs) derived from foundation failures, concrete cracks, and flood overflow in the world. In addition, the hydraulic structures as an essential energy supply system like the power plant must remain operational and functional safety without hydrodynamic instabilities during an earthquake. However, on September 21st, 1999, Chi-Chi earthquake (M_w 7.6) struck critical facilities such as Taipei 101 building, Shih-Kang dam as a concrete gravity dam, and Shih-Kang Primary School located at central region of Taiwan. Taipei 101 building did not suffer any significant structural damage even though it was under construction during the earthquake. On the other hand, Kung et al. [2] observed that the damage of Shih-Kang dam was caused by three different types of failures: (1) structural failure due to large ground motion greater than allowable deformation of the concrete gravity dam; (2) the cracks to weir body and the piers due to strong contact impact; (3) the fracture failure (i.e., one of the most complicated failure types) to the spillways and the abutment of the dam due to combination impact between strong ground motion and fault rupture energy. Besides, analytical studies of seismic evaluation in terms of hydraulic structures

have been issued in recent years, after the unique failure of Shih-Kang dam as a concrete gravity dam structure.

For example, Yao et al. [3] conducted the safety evaluation using seismic fragility of a concrete arch dam located in the southwestern area of China. The seismic fragility was evaluated by nonlinear time history analyses using 18 realistic seismic ground motions. The results from numerical analyses using ABAQUS 3D Finite Element (FE) model noted that the failure criteria such as opening, slipping, and displacement of the dam were affected by seismic ground motions intensity levels. Tekie and Ellingwood [4] used 4 limit states (material failure-concrete, material failure-foundation, sliding at the dam, and deflection of the top of the dam relative to the heel) to develop seismic fragility of concrete gravity dam located on New River in West Virginia in the USA. In particular, the dam-reservoir hydraulic interaction was considered in dynamic equation of motion and spectral accelerations, especially 12 earthquake records which occurred in the USA as intensity measure of ground motions were applied. The numerical results obtained from 2D FE analyses revealed that the sliding at the dam and tensile cracking at the neck of the dam were more critical than other limit states.

Consequently, the seismic safety evaluation of infrastructure (i.e., weir structures) with increase of earthquake records in Korea has received more attention as a key area of research. This study focused on evaluating Probabilistic Seismic Risk Assessment (PSRA) of the weir structure. More specifically, the 2D FE model of the weir structure including soil-structure foundation was conducted by ABAQUS Finite Element package, in order to develop the seismic fragility of the weirs. Furthermore, 30 near-field and 30 far-field earthquake records scaled to different peak ground acceleration (PGA) levels were considered as intensity measure and ground motions uncertainty. In this study, multiple linear time history analyses were carried out to generate the fragility based on Monte Carlo Simulation (MCS).

2. Description of the Weir Structure

The weir structure, Gangjeong-Goryeong weir, designed in 2009 to 2011 is located on the Nakdong River near Daegu Metropolitan City in Korea. This structure was constructed to control the flood and drought, supply the drinking water, and generate the electric power (3000 kW). The overall length of the multifunctional weir system as a concrete gravity structure is 933.5 m. It consists of two different systems: (1) the weir structure (nonoverflow section) with rising sector gates (120 m); (2) another concrete gravity weir system to allow overflow through their tops (833.5 m). The height of each structure is 11 m and the elevation of the two different systems is 9.47 m and 19.50 m, respectively. The storage volume of the system is 92.3 million m^3 and the design flood is 13,200 m^3/s. Moreover, the structure is designed for the maximum flood elevation at 24.02 m. The maintenance range of upstream and downstream of the structure is 300 m and 700 m, respectively, as shown in Figure 1 (http://www.kwater.or.kr/). The soil foundation at the site is classified by three layers: (1) sand layer; (2) gravel-sand mixture layer; (3) rock layer. Figure 2 shows a general design of weirs and the dimensions of overflow monolith (block number 10) at Gangjeong-Goryeong weir structure which is shown in Figure 3.

Figure 1: The maintenance range of upstream and downstream in the Weir (http://www.kwater.or.kr/).

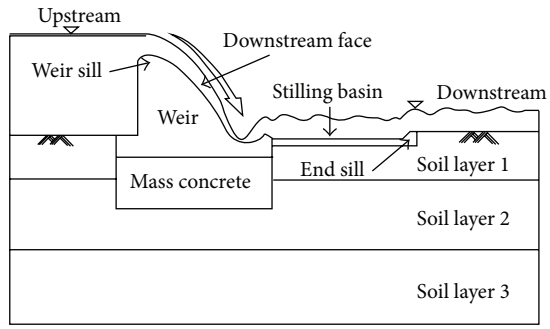

Figure 2: Description of the Gangjeong-Goryeong weir.

Table 1: Material properties of the weir structure.

Structures	Elastic modulus (MPa)	Poisson's ratio	Density (t/mm^3)
Weir body	26,637	0.167	$2.4E-9$
Mass concrete	24,579	0.167	$2.4E-9$
Steel	200,000	0.25	$7.85E-9$
Soil layer 1	2	0.4	$1.7E-9$
Soil layer 1	25	0.4	$1.9E-9$
Soil layer 1	2,000	0.3	$2.4E-9$

3. Finite Element Model of the Weir Structure

3.1. FE Modeling Description. To evaluate the performance of the weir structures, the Finite Element (FE) model was generated by ABAQUS [5], as shown in Figure 4, and a 4-node bilinear plane strain quadrilateral element was applied to the weir body, mass concrete, and soil-structure foundation. The dimension of y direction of the weir system was modeled with 58.114 m and x direction was 83.5 m including upstream and downstream side, in consideration of stress transfer. The material properties for the weir system were listed in Table 1. The design strength of the weir body and mass concrete system designed to peak ground acceleration at 0.154 g was 24 MPa and 18 MPa, respectively, and unit weight was 2350 kg/m^3. For simplification, the weir body as a master surface and mass concrete as a slave surface were connected by tie condition in ABAQUS.

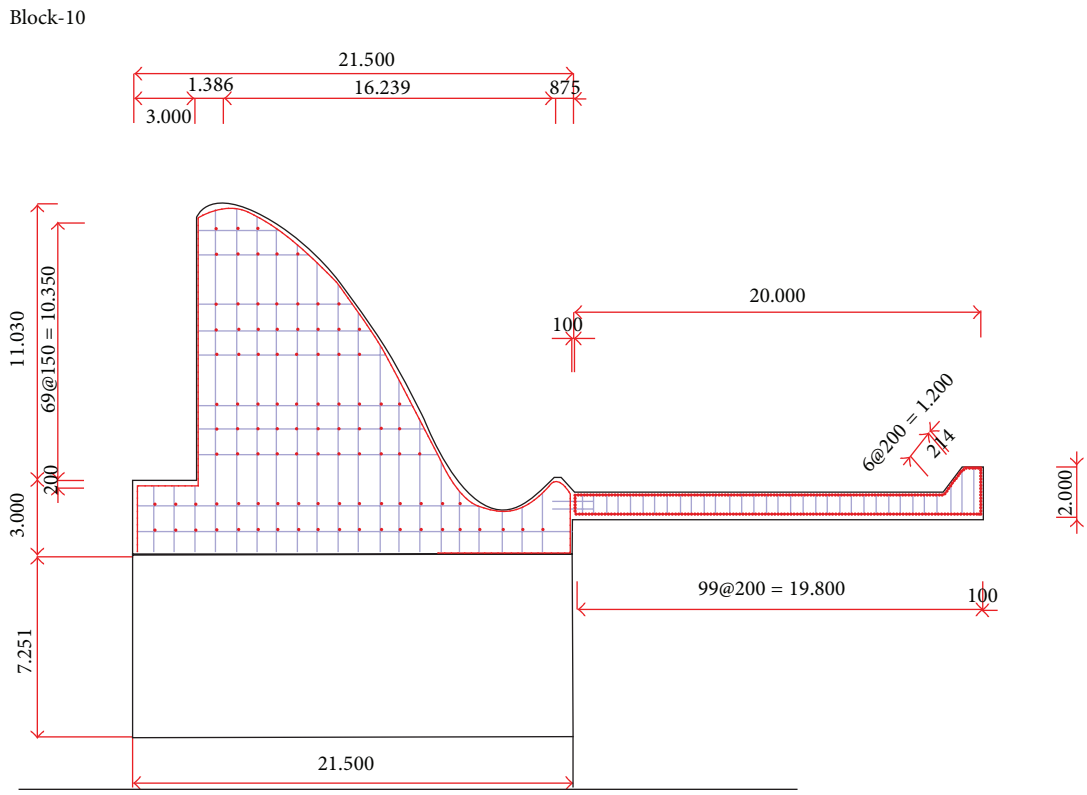

Figure 3: Schematic design of the weir structure (block number 10, unit: mm).

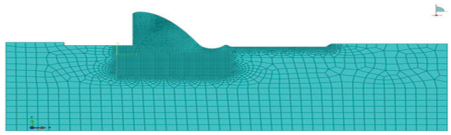

Figure 4: FE model of the weir including soil foundations.

3.2. Loading Conditions. In general, the system weight (gravity-weight) was determined by the combination of concrete unit weight and the system volume and 5 different loading conditions (hydrostatic pressure, hydrodynamic pressure, uplift pressure, silt pressure, and earthquake) were considered in this study. The hydrostatic pressure is typically proportional to the depth of water and the equation of hydrostatic pressure can be expressed as

$$P_w = \gamma_w h, \tag{1}$$

where γ_w = unit weight of water and h is the depth of water. Therefore, the total water pressure in the horizontal direction and vertical water pressure by the unit length are $(1/2)\gamma_w h^2$ and $\gamma_w hA$, respectively.

Next, the weir-reservoir interaction as a hydrodynamic effect was obtained from Westergaard [6] hydrodynamic approach. The mathematical description of hydrodynamic governing equation in two-dimensional system can be derived as follows [6, 7]:

$$\frac{\partial^2 P}{\partial x^2} + \frac{\partial^2 P}{\partial y^2} = \frac{1}{C^2}\frac{\partial^2 P}{\partial t^2}. \tag{2}$$

In this equation, the velocity of sound in water $C = \sqrt{K/\rho_w}$ and $P(x, y, t)$ is the hydrodynamic pressure. ρ_w is the water density and K is the water bulk modulus. In particular, for the structure subjected to an earthquake, the Westergaard hydrodynamic pressure based on added mass method is given as follows:

$$P_d = \frac{7}{8}\rho_w g k \sqrt{H \times h}, \tag{3}$$

where k is $(2/3)(PGA/g)$. H is the total depth of the water and h is the depth from the water surface to the point of hydrodynamic pressure [8].

The uplift pressure of the weir structure is characterized by upward pressure of water as it flows through opening cracks of the foundation or the body connection parts due to the seepage or penetration path [8]. The equation of uplift pressure associated with the hydrostatic pressure may be written as [9]

$$U = \gamma_w \times C \times A \times \left[H_2 + \frac{1}{2}(H_1 - H_2) \times \tau\right], \tag{4}$$

where C is the ratio of area with respect to hydrostatic pressure and A is the bottom area due to uplift pressure. H_1 is

the depth of upstream of the system and H_2 is the depth of downstream of the weir. Also, τ means the ratio of $H_1 - H_2$ in terms of cut-off grouting and drainage curtain.

Besides, earth pressure due to backfill placed against the structure in foundation excavation and silt (horizontal and vertical) pressure due to deposit of silt must be taken into account in the dam or weir design [10]. With dam design criteria in Korea (2011), silt pressure can be calculated by the following:

$$P_s = \gamma_{\text{sub}} K_a H, \tag{5}$$

in which γ_{sub} is the submerged unit weight; K_a defines the coefficient of earth pressure, and H is the depth of silt deposit in the structure.

Lastly, in order to consider the dynamic interaction among the structure, reservoir, and soil-foundation, the dynamic equation of motion of the system subjected to a seismic ground motion can be obtained

$$[m]\{\ddot{u}(t)\} + [c]\{\dot{u}(t)\} + [k]\{u(t)\} = -[m]\left\{\ddot{u}_g(t)\right\} + R, \tag{6}$$

where $\ddot{u}(t)$, $\dot{u}(t)$, and $u(t)$ are the acceleration, velocity, and displacement, $\ddot{u}_g(t)$ is the ground motion, and R is the hydropressure and earth pressure mentioned above. In addition, $[m]$, $[c]$, and $[k]$ are the mass, damping, and stiffness matrices of the system. Details of seismic ground motions for analytical fragility functions of the weir structure are described in the next section.

4. Seismic Ground Motions

In order to develop the seismic vulnerability of the system, the uncertainties of the ground motions with respect to frequency range, ground motion intensity, and earthquake fault mechanism were taken into account. According to Billah et al. [11], the ground motion fault mechanisms as an uncertainty characteristic have a significant effect on the seismic fragility of the bridge. In case of near fault mechanisms, a long period velocity pulse (pulse-like motion) and higher input energy on the system were discharged [11, 12]. Hence, 30-near-field set with epicentral distance less than 10 km and 30-far-field set with epicentral distance over 10 km were carried out to generate the seismic fragility for the weir structure. The details of the ground motions selected from PEER-NGA [13] were listed in Tables 2 and 3.

5. Probabilistic Risk Assessment Methodology: Fragility Function

In recent years, seismic probabilistic risk assessment (SPRA) has been applied to identify the performance and limit/damage state of the systems (nuclear power plants (NPP), bridges, buildings, dams, etc.) in hazard and risk management. Kennedy et al. [14] came out with the seismic fragility as a factor of safe method for NPP and the Electric Power Research Institute (EPRI) [15] developed the assessment of NPP seismic margin using conservative deterministic failure margin methodology to provide in-depth recommendation for the seismic fragility analysis. Moreover, in order to estimate the seismic vulnerability of a bridge structure, various analytical fragility methodologies such as nonlinear time history analyses [16], nonlinear static analyses [17], and Bayesian approach [18] were used. Ellingwood and Tekie [19] and Tekie and Ellingwood [4] presented the safety evaluation of existing concrete gravity dams by reservoir inflow, pool elevation, and spectral acceleration of seismic ground motions. Additionally, Ju et al. [20], Ju and Jung [21], and Ju and Jung [22] carried out Monte Carlo Simulation (MCS) to generate the seismic fragility of piping systems as a nonstructural component in critical facilities. Based on MCS methodology, the conditional probability of failure of the weir structure can be defined as follows:

$$P_f(\text{PGA}) = P[\text{EDPs} > \text{LS} \mid \text{PGA}], \tag{7}$$

in which $P_f(\text{PGA})$ denotes the conditional probability in terms of peak ground acceleration (PGA) as the ground intensity measure. In this study, the displacement and stresses are considered as engineering demand parameters (EDPs) and limit state (LS) is associated with EDPs to construct the fragility. Then, the empirical fragility of the weir structure corresponding to LS given in (8) was obtained from multiple linear time-history analyses using MCS accounting for ground motion uncertainties:

$$P_f(\lambda) = \frac{\sum_{i=1}^{N} (\text{EDPs} \geq \text{LS} \mid \text{PGA} = \lambda)}{\#\text{EQ}_s}, \tag{8}$$

where EDPs are the maximum stress or displacement from ith linear earthquake time-history analysis at a given PGA level. Therefore, the analytical fragility based on MCS for the weir structure in this study can be derived by log-normal cumulative distribution function (CDF) [23]:

$$P_f(\lambda) = \Phi\left[\frac{\ln(\lambda/m_c)}{\beta_{\text{sd}}}\right]. \tag{9}$$

Also, the analytical fragility of the weir structure corresponding to damage states is conducted by a correlation between the median capacity (m_c) and the logarithmic standard deviation (β_{sd}) of the structural system. Therefore, the damage states or limit states must be achieved prior to evaluation of the probability of failure of the system. This study defined the limit states of the weir structure based on Concrete Design Criteria 2003 [24] and Dam Design Criteria 2011 [9] in Korea and five different limit states for the system were presented in Table 4.

6. Seismic Fragility of the Weir Structure

A straightforward elastic FE model of the weir structure including the soil-structure foundation was dealt with for the fragility analyses. Before the evaluation, the analysis of eigenvalues and eigenvectors was conducted, in order to determine the dynamic properties of the weir structure with 5% damping ratio. The damping matrix in this study was determined by Rayleigh damping method in form of [25]

$$[C] = \alpha[M] + \beta[K], \tag{10}$$

Table 2: Selected ground motions: near field.

Number	Events	Year	Station	Mag.	Fault	Epicentral distance (km)	PGA (g)
1	Parkfield	June 28th, 1966	Cholame-Shand on Array number 5	6.19	Strike-slip	9.6	0.1381
2	San Fernando	Feb. 9th, 1971	Pacoima dam	6.61	Reverse	0	1.2259
3	Tabas, Iran	Sep. 16th, 1978	Dayhook	7.35	Reverse	0	0.3279
4	Tabas, Iran	Sep. 16th, 1978	Tabas	7.35	Reverse	1.8	0.8358
5	Imperial Valley	Oct. 15th, 1979	Aeropuerto Mexicali	6.53	Strike-slip	0	0.3267
6	Imperial Valley	Oct. 15th, 1979	El Centro Array number 10	6.53	Strike-slip	6.2	0.1053
7	Imperial Valley	Oct. 15th, 1979	El Centro Array number 4	6.53	Strike-slip	4.9	0.2478
8	Imperial Valley	Oct. 15th, 1979	Sahop Casa Flores	6.53	Strike-slip	9.6	0.2874
9	Victoria, Mexico	June 9th, 1980	Victoria Hospital	6.33	Strike-slip	6.1	0.0446
10	Irpinia, Italy	Nov. 23rd, 1980	Auletta	6.9	Normal	9.5	0.0576
11	Irpinia, Italy	Nov. 23rd, 1980	Bagnoli Irpino	6.9	Normal	8.1	0.1394
12	Irpinia Italy	Nov. 23rd, 1980	Sturno	6.9	Normal	6.8	0.2506
13	Irpinia, Italy	Nov. 23rd, 1980	Calitri	6.9	Normal	8.8	0.1774
14	Morgan Hill	Apr. 24th, 1984	Anderson Dam	6.19	Strike-slip	3.2	0.4230
15	Morgan Hill	Apr. 24th, 1984	Coyote Lake Dam	6.19	Strike-slip	0.2	0.7109
16	Nahanni, Canada	Dec. 23rd, 1985	Site 2	6.76	Reverse	0	0.4890
17	Nahanni, Canada	Dec. 23rd, 1985	Site 3	6.76	Reverse	4.9	0.1404
18	N. Palm Springs	July 08th, 1986	Desert Hot Springs	6.06	Reverse	1.0	0.3313
19	N. Palm Springs	July 08th, 1986	Morongo Valley	6.06	Reverse	3.7	0.2182
20	N. Palm Springs	July 08th, 1986	North Palm Springs	6.06	Reverse	0	0.5941
21	Superstition Hills	Nov. 24th, 1987	Parachute Test Site	6.54	Strike-slip	0.9	0.4550
22	Loma Prieta	Oct. 18th, 1989	Capitola	6.93	Reverse	8.7	0.5285
23	Loma Prieta	Oct. 18th, 1989	Gilroy Gavilan Coll.	6.93	Reverse	9.2	0.3570
24	Loma Prieta	Oct. 18th, 1989	Gilroy Array number 1	6.93	Reverse	8.8	0.2088
25	Chi-Chi Taiwan	Sep. 20th, 1999	CHY006	7.62	Reverse	9.8	0.1301
26	Chi-Chi Taiwan	Sep. 20th, 1999	TCU076	7.62	Reverse	2.8	0.3029
27	Kobe, Japan	Jan. 16th, 1995	Nishi Akashi	6.9	Strike-slip	7.1	0.5093

Table 2: Continued.

Number	Events	Year	Station	Mag.	Fault	Epicentral distance (km)	PGA (g)
28	Kobe, Japan	Jan. 16th, 1995	Takatori	6.9	Strike-slip	1.5	0.6114
29	North Ridge	Jan. 17th, 1994	Newhall	6.69	Reverse	3.2	0.5830
30	North Ridge	Jan. 17th, 1994	Pacoima Kagel Canyon	6.69	Reverse	5.3	0.3011

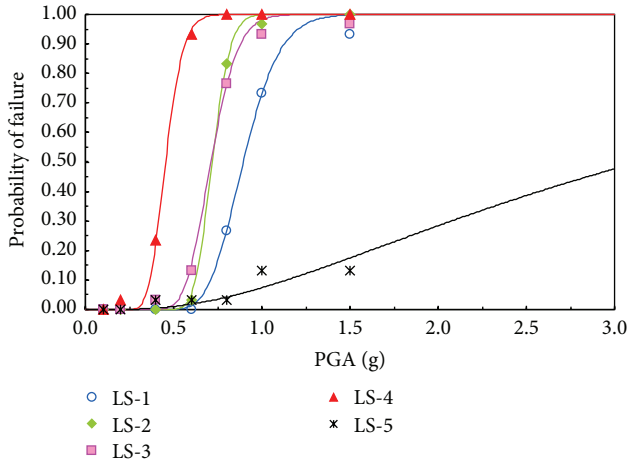

Figure 5: The seismic fragility of the weir subjected to near field ground motions.

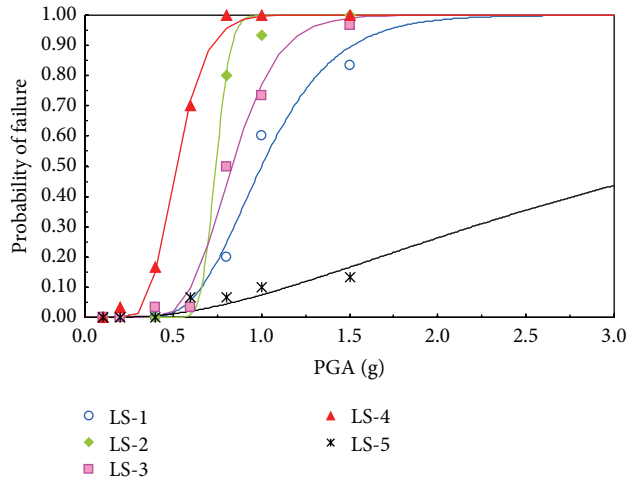

Figure 6: The seismic fragility of the weir subjected to far field ground motions.

where α = the mass constant value and β = the stiffness constant value. Then, the fundamental, second, and third frequencies from the eigenvalues were 0.8911, 1.1223, and 1.2622 Hz, respectively, and about 26% effective mass participation was observed at the third mode. It revealed that the third mode was the largest proportion of the total mass in horizontal direction. Consequently, in the estimation of the fragility of the weir structure, 30-near-field and 30-far-field ground motions normalized to the same PGA levels (0.1 g, 0.2 g, 0.4 g, 0.6 g, 0.8 g, 1.0 g, and 1.5 g) were applied to the simple linear elastic FE model, respectively. In addition, the seismic fragilities were implemented at each PGA using (8) as the empirical method and the analytical seismic fragilities were established by (9) for the Gangjeong-Goryeong weir system. With the multiple time-history analyses accounting for ground motion uncertainties, seismic fragilities corresponding to the limit states were described in Figures 5 and 6. The fragilities noted that the system subjected to ground motions was more vulnerable to the tensile stress of the mass concrete structure than other damages. The similar manner is also observed in the weir system subjected to near field and far field ground motions. The probability of failure due to tensile stress (LS-2) of the weir body was not significantly different from LS-3 (i.e., compressive stress of the mass concrete) in overall PGA levels, as shown in Figure 5. On the other hand, in case of the far field ground motions (Figure 6), the failure difference between LS-2 and LS-3 gradually increased as the seismic hazard level increased. Particularly, it showed that the fragility difference between tensile stress of the weir body and compressive stress of the mass concrete was about 27% at PGA 1.0 g. Also, the relative displacement (LS-5) showed the lowest probability of failure in comparison to other damage states on both ground motions. The fragility comparison for the weir structure subjected to near field and far field ground motion intensity was described in Figures 7 to 11. In comparison to the fragility at limit state 2, the probability of failure of the system presented the similar trend between near field and far field ground motions. In addition, the system subjected to near field ground motions was more vulnerable than the weir structure subjected to far field ground motions. However, the probability of failure of the system at LS-1 due to far field ground motions was higher than that of the system under near field ground motion intensity up to PGA 0.78 g. Therefore, the investigations depicted that the weir structure was sensitive to the ground motion intensity, which was the acceleration-sensitivity structural system.

7. Conclusions

The seismic probabilistic risk assessment, which is the seismic fragility, can be commonly used to identify the performance or characteristic strength of the system at a given seismic

Table 3: Selected ground motions: far field.

Number	Events	Year	Station	Mag.	Fault	Epicentral distance (km)	PGA (g)
1	Kocaeli, Turkey	June 28th, 1999	Ambarli	7.51	Strike-slip	68.1	0.2487
2	San Fernando	Feb. 9th, 1971	Carbon Canyon Dam	6.61	Reverse	61.8	0.0695
3	San Fernando	Feb. 9th, 1971	Cedar Spring	6.61	Reverse	92.2	0.0267
4	San Fernando	Feb. 9th, 1971	Colton	6.61	Reverse	96.8	0.0321
5	San Fernando	Feb. 9th, 1971	Fairmont Dam	6.61	Reverse	25.6	0.0712
6	Friuli, Italy	May 6th, 1976	Barcis	6.5	Reverse	49.1	0.0289
7	Friuli, Italy	May 6th, 1976	Conegliano	6.5	Reverse	80.4	0.0491
8	Irpinia Italy-01	Nov. 23rd, 1980	Rionero in Vulture	6.9	Normal	29.8	0.1059
9	Imperial Valley	Oct 15th, 1979	Calipatria Fire STA	6.53	Strike-slip	23.2	0.1282
10	Imperial Valley	Oct. 15th, 1979	Cerro Prieto	6.53	Strike-slip	15.2	0.1691
11	Irpinia Italy-02	Nov. 23rd, 1980	Mercato San Severino	6.2	Normal	43.5	0.0417
12	Imperial Valley	Oct. 15th, 1979	Compuertas	6.53	Strike-slip	13.5	0.1862
13	Imperial Valley	Oct. 15th 1979	Delta	6.53	Strike-slip	22	0.2378
14	Imperial Valley	Oct. 15th, 1979	Parachute Test Site	6.53	Strike-slip	12.7	0.1113
15	Imperial Valley	Oct. 15th, 1979	Superstition MTN Camera	6.53	Strike-slip	24.6	0.1092
16	Irpinia Italy-02	Nov. 23rd, 1980	Rionero in Vulture	6.2	Normal	22.7	0.0988
17	Chi-Chi Taiwan	Sep. 20th, 1999	CHY019	7.62	Reverse	50	0.0637
18	Chi-Chi Taiwan	Sep. 20th, 1999	CHY022	7.62	Reverse	63.2	0.0443
19	Chi-Chi Taiwan	Sep. 20th, 1999	CHY023	7.62	Reverse	81.1	0.0584
20	Chi-Chi Taiwan	Sep. 20th, 1999	CHY025	7.62	Reverse	19.1	0.1592
21	Kocaeli, Turkey	June 28th, 1999	Arcelik	7.51	Strike-slip	10.6	0.2188
22	Kocaeli, Turkey	June 28th, 1999	Atakoy	7.51	Strike-slip	56.5	0.1048
23	Kocaeli, Turkey	June 28th, 1999	Bursa	7.51	Strike-slip	65.5	0.0453
24	New Zealand 02	Mar. 2nd, 1987	Matahina Dam	6.6	Normal	16.1	0.2553
25	Imperial Valley	Oct. 15th, 1979	El Centro Array number 12	6.53	Strike-slip	17.9	0.0658
26	Imperial Valley	Oct. 15th, 1979	El Centro Array number 13	6.53	Strike-slip	22	0.0456

Table 3: Continued.

Number	Events	Year	Station	Mag.	Fault	Epicentral distance (km)	PGA (g)
27	Imperial Valley	Oct. 15th, 1979	El Centro Array number 3	6.53	Strike-slip	10.8	0.1267
28	Imperial Valley	Oct. 15th, 1979	El Centro Array number 1	6.53	Strike-slip	21.7	0.0564
29	Imperial Valley	Oct. 15th, 1979	El Centro Array number 11	6.53	Strike-slip	12.4	0.1403
30	Parkfield	June 28th, 1966	Temblor Pre-1969	6.19	Strike-slip	17.6	0.3574

Table 4: Limit states of the weir structure.

Limit states	Details	Design criteria
LS-1	Compressive stress at the weir body and stilling basin	$0.25 f_{ck} = 6$ MPa
LS-2	Tensile stress at the weir body and stilling basin	$0.42\sqrt{f_{ck}} = 2.058$ MPa
LS-3	Compressive stress at the mass concrete	$0.25 f_{ck} = 4.5$ MPa
LS-4	Tensile stress at the mass concrete	$0.42\sqrt{f_{ck}} = 1.782$ MPa
LS-5	The displacement of the weir structure	10 mm

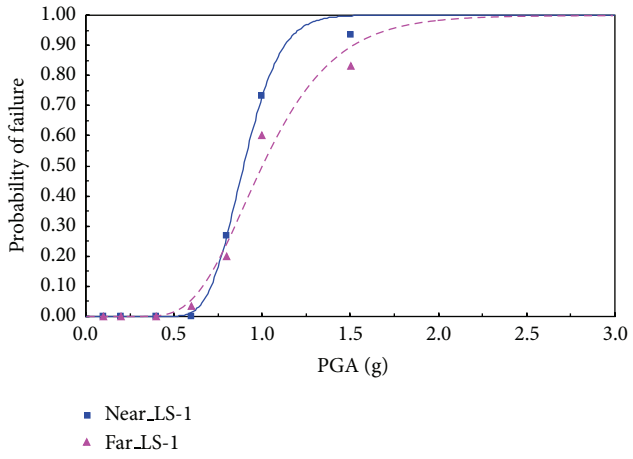

Figure 7: Comparison of the fragility corresponding to LS-1.

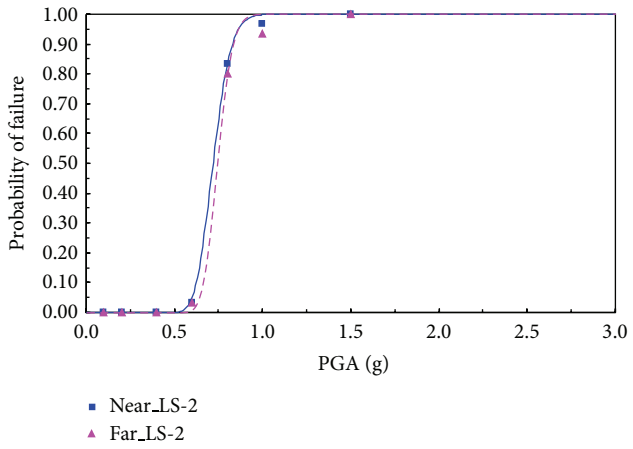

Figure 8: Comparison of the fragility corresponding to LS-2.

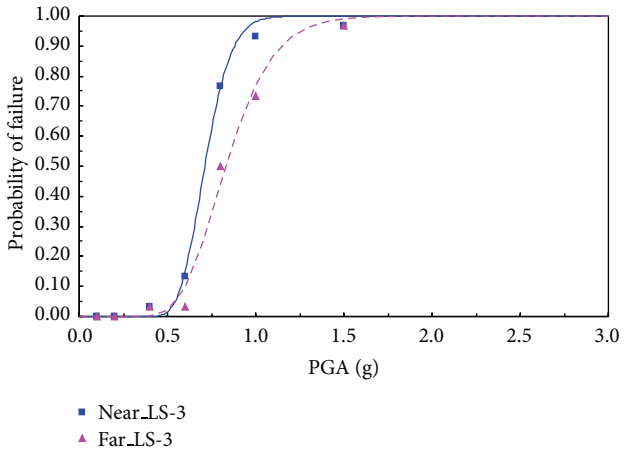

Figure 9: Comparison of the fragility corresponding to LS-3.

hazard level in civil engineering structures. In order to develop the safety assessment for the weir structure as a critical structure in Korea, the fragility analysis was carried out in this study. More specifically, this study developed the simple linear elastic FE model including the soil-structure foundation of Gangjeong-Goryeong weir located on the Nakdong River near Daegu Metropolitan City in Korea. To describe the uncertainty in ground motions of the seismic fragility analyses, near field (30 earthquake records) and far field (30 earthquake records) earthquakes were accounted for as intensity measures. With the particular emphasis on incorporating uncertainty into the 2D plain FE model, multiple linear time history analyses based on MCS were carried out. Through this preprocess, the vulnerability of the weir structure was estimated. As a result, from the eigenvalue

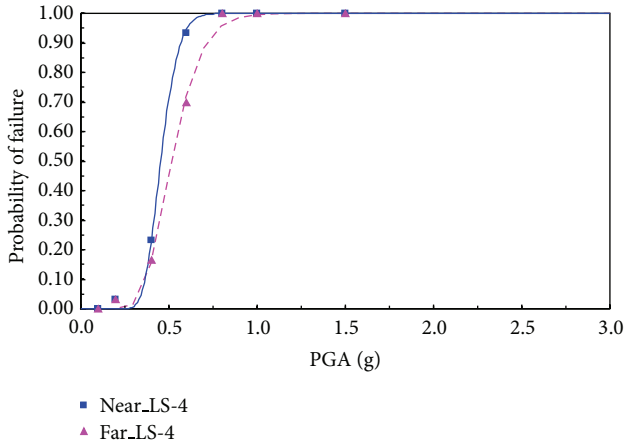

Figure 10: Comparison of the fragility corresponding to LS-4.

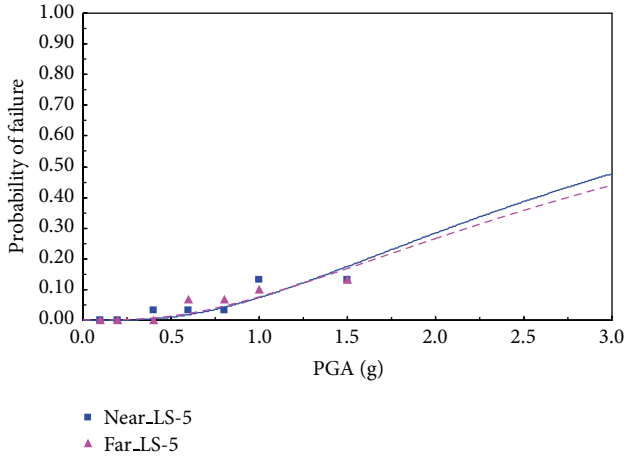

Figure 11: Comparison of the fragility corresponding to LS-5.

analysis, the effective mass participation of the third mode in the weir structure was significantly larger than that of the first mode and the second mode in horizontal direction. It was noted that the mode shape and mass participation were very different from the typical building type. The empirical and analytical fragility results in particular revealed that the weir structure was more conservative to the near field fault mechanism in comparison to the far field fault. Furthermore, the weir system including mass concrete and soil foundations was relatively susceptible to limit state 4 (tensile stress at the mass concrete) as compared to other damage states, during an earthquake.

Finally, the seismic fragility accounting for the nonlinearity with respect to the interaction between the weir body and soil-structure foundation must be achieved and for a future safety assessment of the weir system the effect of flooding condition must be also considered.

Conflict of Interests

The authors declare that there is no conflict of interests regarding the publication of this paper.

Acknowledgments

This research was supported by a Grant (14SCIP-B065985-02) from Smart Civil Infrastructure Research Program funded by Ministry of Land, Infrastructure and Transport (MOLIT) of Korea government and Korea Agency for Infrastructure Technology Advancement (KAIA).

References

[1] H. Chanson, "A review of accidents and failures of stepped spillways and weirs," *Proceedings of the Institution of Civil Engineers: Water and Maritime Engineering*, vol. 142, no. 4, pp. 177–188, 2000.

[2] C. S. Kung, W. P. Ni, and Y. J. Chiang, "Damage and rehabilitation work of Shih-Kang dam," in *Proceedings of the Seismic Fault-Induced Failures Workshop*, pp. 33–48, 2001, http://shake.iis.u-tokyo.ac.jp/seismic-fault/workshops/papers/03.PDF.

[3] X. W. Yao, A. S. Elnashai, and J. Q. Jiang, "Analytical seismic fragility analysis of concrete arch dams," in *Proceedings of the 15th World Conference on Earthquake Engineering*, Lisbon, Portugal, September 2012.

[4] P. B. Tekie and B. R. Ellingwood, "Seismic fragility assessment of concrete gravity dams," *Earthquake Engineering and Structural Dynamics*, vol. 32, no. 14, pp. 2221–2240, 2003.

[5] ABAQUS, "Ver 6.13, Dassault Systemes".

[6] H. M. Westergaard, "Water pressure on dams during earthquakes," *Transactions of the ASCE*, vol. 98, pp. 418–433, 1933.

[7] P. Chakrabarti and K. Chopra, "Earthquake analysis of gravity dams including hydrodynamic interaction," *Earthquake Engineering and Structural Dynamics*, vol. 2, no. 2, pp. 143–160, 1973.

[8] A. Rasekh, "Hydrodynamic pressure on culvert gates during an earthquake," in *Proceedings of the SIMULA Community Conference*, pp. 1–13, 2012.

[9] *Dam Design Criteria in Korea*, Ministry of Land, Infrastructure and Transport, 2011.

[10] R. S. Jansen, *Advanced Dam Engineering for Design, Construction, and Rehabilitation* , Van Nustrand Reinhold, New York, NY, USA, 115th edition, 1988.

[11] A. H. M. M. Billah, M. S. Alam, and M. A. R. Bhuiyan, "Fragility analysis of retrofitted multicolumn bridge bent subjected to near-fault and far-field ground motion," *Journal of Bridge Engineering, ASCE*, vol. 18, no. 10, pp. 992–1004, 2013.

[12] P. G. Somerville, "Characterizing near fault ground motion for the design and evaluation of bridges," in *Proceedings of the 3rd National Conference and Workshop on Bridges and Highways*, Portland, Ore, USA, 2002.

[13] PEER-NGA, Pacific Earthquake Engineering Research Center: NGA Database, http://peer.berkeley.edu/nga/.

[14] R. P. Kennedy, C. A. Cornell, R. D. Campbell, S. Kaplan, and H. F. Perla, "Probabilistic seismic safety study of an existing nuclear power plant," *Nuclear Engineering and Design*, vol. 59, no. 2, pp. 315–338, 1980.

[15] Electric Power Research Institute (EPRI), "Methodology for developing seismic fragilities," Research Project TR-103959, 1994.

[16] J. Park and E. Choi, "Fragility analysis of track-on steel-plate-girder railway bridges in Korea," *Engineering Structures*, vol. 33, no. 3, pp. 696–705, 2011.

[17] M. Shinozuka, M. Q. Feng, H.-K. Kim, and S.-H. Kim, "Nonlinear static procedure for fragility curve development," *Journal of Engineering Mechanics*, vol. 126, no. 12, pp. 1287–1295, 2000.

[18] J. Li, B. F. Spencer, and A. S. Elnashai, "Bayesian updating of fragility functions using hybrid simulation," *Journal of Structural Engineering*, vol. 139, no. 7, pp. 1160–1171, 2013.

[19] B. Ellingwood and P. B. Tekie, "Fragility analysis of concrete gravity dams," *Journal of Infrastructure Systems*, vol. 7, no. 2, pp. 41–48, 2001.

[20] B. S. Ju, S. K. Tadinada, and A. Gupta, "Fragility analysis of threaded T-joint connections in hospital piping systems," in *Proceedings of the Pressure Vessels and Piping Conference (PVP '11)*, pp. 147–155, Baltimore, Md, USA, July 2011.

[21] B. S. Ju and W. Y. Jung, "Seismic fragility evaluation of multi-branch piping systems installed in critical low-rise buildings," *Disaster Advances*, vol. 6, no. 4, pp. 59–65, 2013.

[22] B. S. Ju and W. Y. Jung, "Probabilistic risk assessment: piping fragility due to earthquake fault mechanisms," *Mathematical Problems in Engineering*. In press.

[23] R. P. Kennedy and M. K. Ravindra, "Seismic fragilities for nuclear power plant risk studies," *Nuclear Engineering and Design*, vol. 79, no. 1, pp. 47–68, 1984.

[24] *Concrete Design Criteria in Korea*, Korea Concrete Institute, 2003.

[25] A. K. Chopra, *Dynamics of Structures*, Prentice Hall, Upper Saddle River, NJ, USA, 2nd edition, 2007.